Effects of molecular asymmetry of optically active molecules on the polarization properties of multiply scattered light

I. Alex Vitkin
Department of Medical Biophysics and Radiation Oncology, Princess Margaret Hospital / Ontario Cancer Institute / University Health Network and the University of Toronto, Toronto, Ontario, Canada M5G 2M9

Richard D. Laszlo
Department of Physics, Queen's University, Kingston, Ontario, Canada K7L 3N6

Claire L. Whyman
Department of Physics, University of Waterloo, Waterloo, Ontario, Canada N2L 3G1

Abstract: The use of polarized light for investigation of optically turbid systems has generated much recent interest since it has been shown that multiple scattering does not fully scramble the incident polarization states. It is possible under some conditions to measure polarization signals in diffusely scattered light, and use this information to characterize the structure or composition of the turbid medium. Furthermore, the idea of quantitative detection of optically active (chiral) molecules contained in such a system is attractive, particularly in clinical medicine where it may contribute to the development of a non-invasive method of glucose sensing in diabetic patients. This study uses polarization modulation and synchronous detection in the perpendicular and in the exact backscattering orientations to detect scattered light from liquid turbid samples containing varying amounts of L and D (left and right) isomeric forms of a chiral sugar. Polarization preservation increased with chiral concentrations in both orientations. In the perpendicular orientation, the optical rotation of the linearly polarized fraction also increased with the concentration of chiral solute, but in different directions for the two isomeric forms. There was no observed optical rotation in the exact backscattering geometry for either isomer. The presence of the chiral species is thus manifest in both detection directions, but the sense of the chiral asymmetry is not resolvable in retro-reflection. The experiments show that useful information may be extracted from turbid chiral samples using polarized light.

OCIS codes: (290.4210) Multiple Scattering; (290.7050) Turbid Media; (260.2130) Ellipsometry and Polarimetry

References and Links

1. L. D. Barron, *Molecular Light Scattering and Optical Activity* (Cambridge Press, London, 1982).
2. M. P. van Albada and A. Lagendijk, "Observation of weak localization of light in a random medium," Phys. Rev. Lett. 55, 2692-2695 (1985).
3. P.E. Wolf and G. Maret, " Weak localization and coherent backscattering of photons in disordered media," Phys. Rev. Lett. **55**, 2696-2699 (1985).
4. J. M. Schmitt, A. H. Gangjbakhche, and R. F. Bonner, "Use of polarized light to discriminate short-path photons in multiply scattering medium," Appl. Opt. **31**, 6535-6546 (1992).
5. M. P. Silverman, W. Strange, J. Badoz, and I. A. Vitkin, " Enhanced optical rotation and diminished depolarization in diffusive scattering from a chiral liquid," Opt. Commun. **132**, 410-416 (1996).
6. Vitkin and E. Hoskinson, "Polarization studies in multiply scattering chiral media," Opt. Eng. **39**, 353-362 (2000).

#696 - $15.00 US Received January 07, 2002; Revised February 21, 2002

7. R. C. N. Studinski and I. A. Vitkin, "Methodology for examining polarized light interactions with tissues and tissuelike media in the exact backscattering direction," J. Biomed. Opt. **5**, 330-337 (2000).
8. X. Wang, G. Yao, and L. H. Wang, "Monte Carlo model and single-scattering approximation of the propagation of polarized light in turbid media containing glucose," Appl. Opt. **41**, 792-801 (2001).
9. Hielscher, J. R. Mourant, and I. J. Bigio, "Influence of the particle size and concentration on the diffuse backscattering of polarized light from tissue samples and biological cell suspensions," Appl. Opt. **36**, 125-135 (1997).
10. M. J. Rakovic and G. W. Kattawar, "Theoretical analysis of polarization patterns from incoherent backscattering of light," Appl. Opt. **37**, 3333-3338 (1998).
11. G. Yao and L. H. Wong, "Two-dimensional depth-resolved Mueller matrix characterization of biological tissue by optical coherence tomography," Opt. Lett. **24**, 537-539 (1999).
12. S. Bartel and A. H. Hielscher, "Monte Carlo simulations of the diffuse backscattering Mueller matrix for highly scattering media," Appl. Opt. **39**, 1580-1588 (2000).
13. H. Hilescher, A. A. Eick, J. R. Mourant, D. Shen, J. P. Freyer, and I. J. Bigio, "Diffuse backscattering Mueller matrices of highly scattering media," Opt. Express **1**, 441-454 (1997), http://www.opticsexpress.org/abstract.cfm?URI=OPEX-1-13-441
14. Ambirajan and D. C. Look, "A backward Monte Carlo study of the multiple scattering of a polarized light beam," J. Quant. Spectrosc. Radiat. Transfer **58**, 171-192 (1997).
15. V. Sankaran, J. T. Walsh, and D. J. Maitland, "Polarized light propagation through tissue phantoms containing closely packed scatterers," Opt. Lett. **25**, 239-241 (2000).
16. V. Sankaran, M. J. Everett, D. J. Maitland, and J. T. Walsh, "Comparison of polarized light propagation in biological tissues and phantoms," Opt. Lett. **24**, 1046-1048 (1999).
17. S. L. Jacques, J. R. Roman, and K. Lee, "Imaging superficial tissues with polarized light," Lasers Surg. Med. **26**, 199-129 (2000).
18. J. McNickols and G. L. Cote, "Optical glucose sensing in biological fluids: an overview," J. Biomed. Opt. **5**, 5-16 (2000).
19. J. C. Kemp, "Piezo-optical birefringence modulators: new use for a long-known effect," J. Exp. Theor. Phys. **59**, 950-954 (1969).
20. E. Collett, *Polarized Light: Fundamentals and Applications* (Marcel Dekker, New York, 1993).
21. C. Brosseau, *Fundamentals of Polarized Light: a Statistical Optics Approach* (Wiley, New York, 1998).
22. K. Hadley and I. A. Vitkin, "Linear and circular depolarization rates in diffusive scattering from chiral, achiral, and racemic turbid media," J. Biomed. Optics (submitted Feb 2002).
23. A.S. Martinez and R. Maynard, "Polarization statistics in multiple scattering of light: a Monte Carlo approach," in: C. M. Soukoulis (ed.) *Photonic Band Gaps and Localization*, 99-114 (Plenum, New York, 1993).
24. Lakhtakia, *Beltrami Fields in Chiral Media* (World Scientific Publishing, Singapore, 1994).
25. D. Bicout, C. Brosseau, A. S. Martinez, and J. M. Schmitt, "Depolarization of multiply scattered waves by spherical diffusers: influence of size parameter," Phys. Rev. E **49**, 1767-1770 (1994).

Introduction

Chiral molecules exhibit structural asymmetry that can be sensed with optical polarization techniques. For example, upon transmission through a transparent sugar solution, the polarization plane of linearly polarized light is rotated about the propagation direction by an amount dependent on the thickness of the medium, the concentration of the dissolved chiral sugar, and its specific rotatory power at the measurement wavelength. This effect is caused by the circular birefringence of the transparent sugar solution. The sense of rotation depends on the isomeric form of the dissolved chiral species; for example, if D-glucose is seen to rotate the polarization plane of the transmitted light in the counter-clockwise direction, then its isomeric opposite, L-glucose, will rotate the polarization plane by an equal amount in the clockwise direction. These and other chiral asymmetries, such as linear birefringence and circular dichroism, are well known and readily measured in optically transparent or translucent materials [1].

Detection of chiral asymmetries in optically turbid random media using polarized light methods is much more difficult. Since multiple scattering is an effective depolarization mechanism, polarization investigations of turbid systems (chiral or achiral) is compromised. In fact, only in the last two decades has it been conclusively shown that partial polarization preservation is measurable in these systems under some experimental conditions [2-4]. Further, we and others have recently reported the detection of chiral asymmetries in diffusive scattering from turbid chiral samples [5-7]. Several research groups have also developed

#696 - $15.00 US Received January 07, 2002; Revised February 21, 2002

experimental and theoretical methods to investigate polarized light propagation in turbid synthetic or biological media, in an attempt to understand the mechanisms of depolarization, quantify relevant depolarization scales, derive the system Mueller matrices, and account for the presence of glucose [8-17]. In addition to their potential scientific merit, these initial findings may have important implications in biomedical optics, particularly in devising a non-invasive means for glucose monitoring in diabetic patients. The highly scattering nature of most mammalian tissues has so far thwarted attempts to develop a non-invasive glucose monitoring system based, among others, on reflectance spectroscopy, fluorescence, or Raman effects [18]. It remains to be determined whether glucose detection in turbid tissues using polarized light will prove sufficiently sensitive and specific to impact the outstanding clinical problem. The work presented below is part of our continuing effort aimed at this determination.

In this publication, we use polarization modulation and synchronous detection methods to examine the effects of L and D isomers of sugar dissolved in a water solution containing scattering polystyrene microspheres. We derive the optical rotation and the degree of polarization parameters from measurements at 90^o and 180^o to the incident beam. The dependence of these derived parameters on the chirality and turbidity of the medium is examined.

Experimental

Figure 1 shows the schematic of the experimental setup for polarization measurements in both the perpendicular and the exact backscattering orientations. Light emitted from a 633 nm HeNe laser passed through a polarizer set to 45° with respect to the optical table, followed by a mechanical chopper operating at 135 Hz. A lock-in amplifier tuned to the chopper frequency can record a signal proportional to the overall light intensity S_{dc}, as required in the theoretical derivations below. The light then traversed through the transparent quartz oscillator of the photoelastic modulator (PEM) that imparted a time-varying polarization to the passing beam [19]. The PEM is a resonant device operating at a frequency of 50 kHz; its oscillation axis was horizontal, with a with a peak retardation value set to δ_o=3.469 rad in order to maximize the Bessel function coefficients of the detected signal harmonics. To ensure that there are no interference effects caused by multiple reflections from the surfaces of the PEM quartz element, it was angled by ~6^o in the horizontal plane off perpendicular to the light propagation direction.

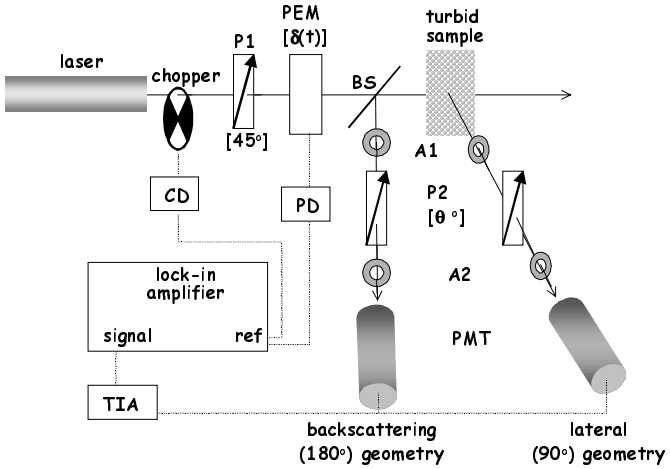

Figure 1: Schematic of the polarization measurement apparatus, showing both perpendicular (90^o) and exact backscattering (180^o) detection geometries. P's = linear polarizers; A's = apertures; PEM = photoelastic modulator; PMT = photomultiplier tube; TIA = transimpedance amplifier; CD = chopper driver (135 Hz); PD = PEM driver (50 kHz).

#696 - $15.00 US Received January 07, 2002; Revised February 21, 2002

In the perpendicular detection direction, light exiting the quartz element of the PEM impinged on the sample under test. The light diffusely reflected at 90^o to the incident beam then passed through a pair of iris diaphragms, traversed through another linear polarizer (analyzer) with its pass axis variable (angle θ in the expressions below, varied from 30° to 150° in 10 degree increments), and was detected by a photomultiplier tube (PMT). The photocurrent from the PMT was filtered and converted to a voltage signal by a transimpedance preamplifier. A lock-in amplifier measured the signals at both chopper frequency (135 Hz ~ S_{dc}) and at twice the PEM modulation frequency (100 kHz ~ S_{2f}). The S_{2f}/S_{dc} ratio was calculated at each angle of the analyzer θ, and scaled by a correction factor that converted the rms lock-in measurements to true peak-to-peak ratios for comparison with the theoretical expression. The corrected ratios and the corresponding analyzer angles were input into the non-linear regression analysis package (SigmaPlot 3.0), which determined the sample optical rotation (α) and degree of polarization (β) that minimized the sum of the squared differences between theory and measurements.

To measure polarization effects in the exact back-scattering direction, the set-up was modified slightly. A 45^o glass beam splitter was placed between the PEM and the sample, to reflect a fraction of the retro-reflected sample light toward the detector assembly (consisting, as above, of the two apertures, the analyzer, and PMT). For these measurements, the analyzer angle was varied from 90° to 270° in 10 and 15 degree increments. This range is different from that used in the perpendicular detection geometry; both ranges were selected to pick out regions of greatest signal variation [Eqs. (1) and (2) below] in order to optimize sensitivity in the respective data fits.

A mirror was used to check the consistency of the theory in the backscattering direction, and to ensure that the system was aligned and calibrated properly. The mirror positioned perpendicular to the beam is a good control sample because its parameters α and β should have values of 0 and 1, respectively. Once good agreement with these expected values was achieved (typically $\alpha=0.0\pm0.1^o$, $\beta=(100.0\pm0.1)\%$, with a goodness of fit R^2 value of >0.999), the system was used for measuring the turbid chiral samples. These consisted of 1.4 μm-diameter polystyrene microspheres suspended in deionized water at 0.21 (mass/vol) concentration, with varying amounts of the two isomeric forms of chiral solute. A logical choice for the latter would be glucose; however, it occurs naturally only in its D-isomeric form, so its L-counterpart is exceedingly rare and expensive. A similar chiral plant sugar, arabinose, is available readily in both L and D forms, and was thus used for this study. Its concentration range in the 0.21% microsphere suspensions was 0-1.2M, with three intermediate molarities examined. All samples had errors in concentration of ±0.005M. The sample scattering coefficients were calculated from Mie theory. Using $n_{spheres}=1.575$, $n_{water}=1.33$, and accounting for the water refractive index elevation due to dissolved arabinose (+0.022/M, measured with a refractometer), there results for the 0M sample: scattering coefficient $\mu_s=77.4\ cm^{-1}$, scattering anisotropy g=0.936, transport scattering coefficient $\mu_s'=\mu_s(1-g)=4.9\ cm^{-1}$. The samples thus exhibit significant turbidity and highly forward-peaked scattering anisotropy. For the same microsphere concentration but at the highest examined molarity of 1.2M, $\mu_s=69.2\ cm^{-1}$, g=0.945, and $\mu_s'=\mu_s(1-g)=3.8\ cm^{-1}$. The reduction of the medium turbidity at fixed scatterer concentration due to dissolved arabinose is non-negligible, of the order of 10-20% for the range of samples examined in this work.

The samples were contained in a rectangular (1cm x 1cm) optical grade quartz cuvette. For the back-scattering measurements, the cuvette was angled slightly to ensure that the specularly reflected spot did not reach the detector. Extreme care was taken while a set of measurements was being acquired to keep all instrumentation and optics consistent. Special attention was paid to reproducibly positioning the cuvette between samples, especially in the back-scattering direction. The data was acquired at room temperature.

#696 - $15.00 US Received January 07, 2002; Revised February 21, 2002

Theory

The theoretical models that simulate the interaction of different polarization states with the turbid chiral medium in the two detection directions have been described previously [6,7]. Briefly, each element in the beam path is modeled by a 4x4 Mueller matrix, which multiplies the Stokes vector of the incident light to represent the resulting interaction. The Mueller matrices of the experimental elements can be found in standard textbooks [20,21]. The sample is modeled as an optical rotator (described by the optical rotation α, to account for chirality) and a depolarizer (described by the degree of polarization β, to account for turbidity); in the back-scattering direction, a retro-reflector matrix is also included. While in general matrices do not commute, the effect of varying their present multiplication order is only to change the sign of the α parameter (i.e., α becomes $-\alpha$), and this is unimportant for the current study. The depolarizer matrix can either be isotropic or non-isotropic (same versus different depolarization rates for linear and circular polarizations); for this work, the two formalisms are equivalent since the circular depolarization rate, whether same or different from the β above, does not propagate to the final signal expressions of Equations (1) and (2). Alternate arrangements of the analyzing polarization optics that can explicitly differentiate between linear and circular depolarization contributions will be investigated in a separate study [22].

The expression for the first element of the final Stokes vector yields the intensity of the light entering the photodetector. By expanding in Bessel function harmonics, the signal at the 2^n harmonic of the PEM modulation frequency, normalized by the overall light intensity, becomes (in the perpendicular orientation)

$$\frac{S_{2f}}{S_{dc}}(\perp) = \frac{2\beta J_2(\delta_o)\sin 2(\alpha+\theta)}{1+\beta J_o(\delta_o)\sin(\alpha+\theta)} \qquad (1)$$

where J_2 and J_o are the second-order and zeroth-order Bessel functions evaluated at the maximum PEM retardation setting of δ_o, and θ is the analyzer angle varied in the experiment that acts as the independent variable in the regression fit to determine sample α and β.

The experiments in the exact backscattering direction employed a beamsplitter, introducing both transmission and reflection matrices that complicate the resulting expression considerably, but do enable measurements at 180^o to the incident beam. This is particularly important: in contrast to all other orientations, one expects a non-vanishing polarization signal even for infinitely thick turbid media. This effect in the exact backscattering direction has been explained in terms of weak localization mechanism [2,3,21,23]. For our arrangement, there results

$$\frac{S_{2f}}{S_{dc}}(\Leftrightarrow) = \frac{2J_2(\delta_o)A}{J_o(\delta_o)A+B+C} \qquad (2)$$

$$A = 1.82\beta[0.58\cos(2\alpha)\sin(2(\theta+90)) - \sin(2\alpha)\cos(2(\theta+90)) - 0.82\sin(2\alpha)]$$

$$B = 1.82[1+0.82\cos(2(\theta+90))]$$

$$C = -0.176\beta[\{0.815+\cos(2\alpha)\cos(2(\theta+90))\} - 0.102\sin(2\alpha)\sin(2(\theta+90))]$$

The numerical values in Eq. (2) are derived from Snel's law, assuming a 45^o glass beamsplitter with n_{BS}=1.54.

#696 - $15.00 US Received January 07, 2002; Revised February 21, 2002

Results and Discussion

Typical results measured at 90° from a turbid sample containing 0.21% (mass/vol) microspheres and 0.38M L-arabinose are shown in Figure 2(a). The data points are the corrected S_{2f}/S_{dc} ratio plotted against analyzer angle θ. The resulting fit using equation (1) yields an optical rotation α of 0.53±0.18° and a polarization preservation β of (33.3±0.2)%, with a goodness of fit R^2 value of 0.99941. All the measurements gathered in the perpendicular orientation were in excellent agreement with the theoretical model, with $R^2 >$ 0.999, and small errors in both α (< ±5%) and β (< ±1%).

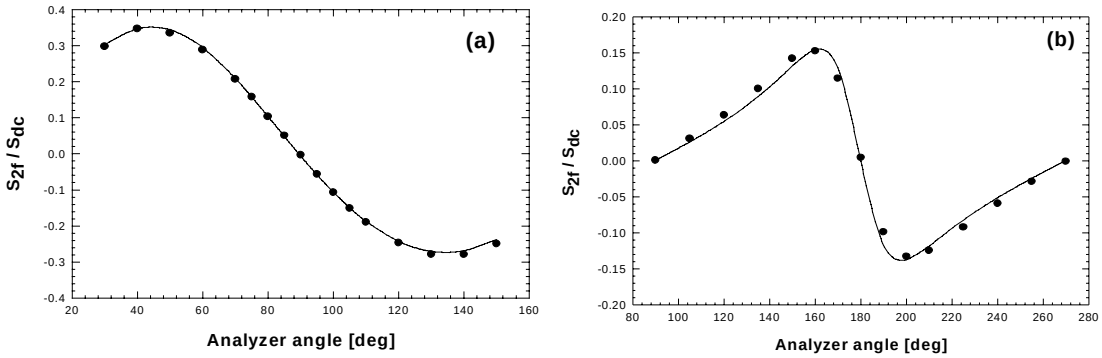

Figure 2: **(a)** Typical data set and analytical fit from Equation (1) for a sample containing 0.38M L arabinose with 0.21% microspheres in the perpendicular orientation. Points represent scaled experimental data ratios while the smooth curve is the theoretical fit, described by α=0.53±0.18° and β=(33.3±0.2)%, with a goodness of fit R^2=0.99941. **(b)** Typical data set and analytical fit from Equation (2) for a sample containing 0.52M L arabinose with 0.21% microspheres in the backscattering orientation. The fit is optimal for α=-0.12 ±0.60° and β=(15.9±0.4)%, with R^2=0.9922.

The added difficulty of the measurement and the complexity of the theoretical fit make the backscattering results slightly more uncertain, as reflected in the quality of the data compared to the perpendicular detection geometry. A typical result from a sample containing 0.21% microspheres and 0.52M L arabinose is depicted in Figure 2(b). The fit using equation (2) gives α=-0.12±0.60°, β=(15.9±0.4)%, R^2=0.9922. Most backscattering results had R^2 values between 0.98 and 0.995, with correspondingly larger errors in the fitted parameters than in the perpendicular setup.

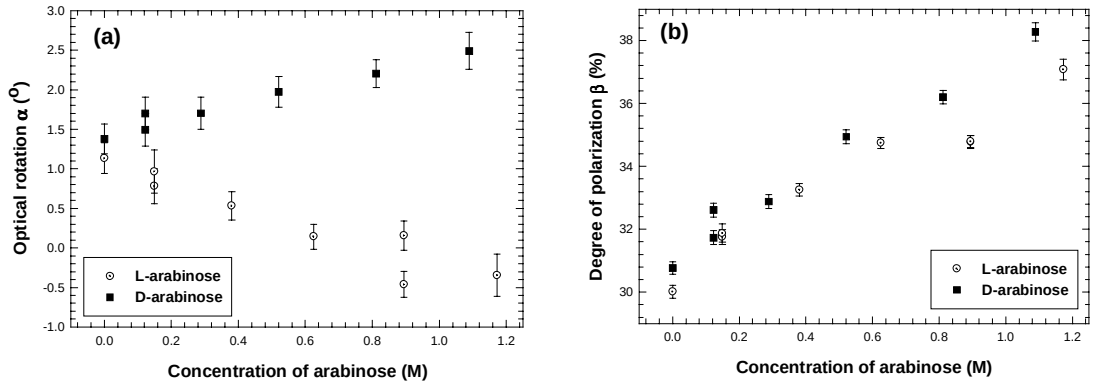

Figure 3: **(a)** Induced optical rotation as a function of concentration of L and D forms of arabinose in solutions containing 0.21% microspheres, measured in the perpendicular direction. Error bars represent regression-fit uncertainties in derived parameters. Selected reproducibility results from repeated measurements are also displayed. **(b)** Degree of polarization as a function of concentration of L and D forms of arabinose, derived from the same experimental sets as the results of 3(a).

#696 - $15.00 US Received January 07, 2002; Revised February 21, 2002

Figure 3(a) shows the dependence of the derived optical rotation on the molar concentration of L and D forms of arabinose measured at 90^o to the incident beam. The error bars are the standard deviations of a particular non-linear regression fit (as in Figure 2(a)), and are about equal to the reproducibility errors obtained on repeated measurements. A clear increase in the magnitude of the induced optical rotation is observed with increasing concentrations of both varieties of arabinose. Furthermore, the two isomers display a rotation of the linear polarization in opposite directions, providing strong evidence that the current methodology can detect the sense of the molecular asymmetry of the chiral solute. Also evident is the offset in the optical rotation for the 0M sample of $\sim 1^o$. The fact that the curves do not start at the origin suggests that either the microspheres or the cuvette were contributing to the induced optical rotation, or the calibration / alignment procedures were introducing some systematic errors. The cause of this minor discrepancy is currently unresolved.

Figure 3(b) is the corresponding plot of the degree of polarization versus arabinose concentrations, derived from the same data sets as the graph in Figure 3(a). As expected, β does not depend on the isomeric form of sugar used, as the results are essentially the same for both L and D chiral samples. The values of β are at a minimum of ~30% for the 0M suspension and increase monotonically with increasing arabinose concentration to ~38% for the 1.18M sample. The increase in the polarization preservation may be due to the simple effect of arabinose-induced refractive index matching, whereby the scattering coefficient decreases with increasing arabinose concentration in suspensions containing a fixed number of scatterers. As detailed above, there is a 11% decrease in μ_s (and a 19% decrease in μ_s') over the 0M-1.2M range, which may cause the ~30% $\rightarrow$ 38% increase in β. Alternatively, the actual chirality of the medium could be responsible: the propagation EM eigenmodes in chiral systems are circular polarization states [24], and circular polarization has been shown to be preferentially preserved in a medium with strong forward anisotropic scattering [4-6,21,25].

The stringent requirements in optical alignment and the weaker signals resulting from the beamsplitter reflection make accurate measurements in the backscattering orientation difficult. To account for the experimental uncertainties in this orientation, several sets of data were taken over several days. The values shown in the graphs of Figure 4 are the mean values from those sets, with the error bars representing one standard deviation from the mean. Data for the two chiral isomers were indistinguishable from each other, so results from both L and D experiments were averaged together.

Figure 4(a) shows that neither the concentration of arabinose nor its isomeric form affect the induced optical rotation of the diffusely scattered light in the exact backscattering direction. This may be caused by the retro-reflection of the beam along the same zig-zag path as the incident beam, inducing an equal and opposite counter-rotation and yielding a net measured rotation of $\sim 0^o$. Although a similar system has been reported to have a non-negligible optical rotation in the near-backscattering direction ($\sim 6^o$ away from retroreflection) [5], this is the first unambiguous null result for PEM-measured optical rotation at exactly 180^o to the incident beam.

The dependence of polarization preservation on arabinose concentration in the exact backscattering direction is qualitatively similar to the findings at the perpendicular orientation. The percentage of polarization information preserved increases with increasing sugar concentration, with results independent of the chiral form of arabinose. Values of β varied from (15±3)% for the sample containing no sugar to (26±5)% for the 1.08M solution. It is interesting to note that for these turbid samples, the lateral direction measurements resulted in larger polarization preservation than obtained in the backscattering direction. This trend depends on the magnitude of the scattering coefficient; however, with increasing turbidity, only the measurements in the exact backscattering direction will yield a non-zero value for β [21,23]. The scientific and clinical significance of this observation is currently being examined.

#696 - $15.00 US Received January 07, 2002; Revised February 21, 2002

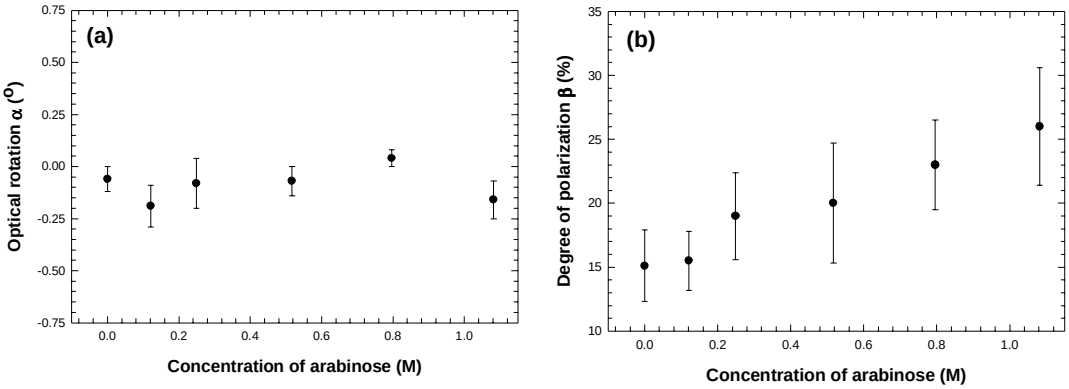

Figure 4: **(a)** Mean optical rotation as a function of concentration of arabinose in solutions containing 0.21% microspheres in the backscattering orientation. The points are the means of the four separately derived α's (two from L and two from D measurements), and the error bars represent the standard deviations of the means. **(b)** Corresponding mean backscattering results for the degree of polarization. Meaning of symbols and error bars is the same as in 4(a).

Conclusion

We have measured the effect of chiral asymmetries in diffusive scattering from a turbid fluid using polarization modulation and synchronous detection techniques. In both perpendicular and backscattering detections, the surviving degree of polarization was found to increase with increasing arabinose concentration independent of its isomeric form. Whether this is caused by the sugar-induced refractive index-matching effect, or stems from the chiral nature of the solute, is currenty unclear. Studies using chiral solutions, achiral solutions, and racemic (L/D) mixtures all with the same refractive indexes are underway to answer this fundamental question [22]. The corresponding optical rotations were distinguishable for the two isomeric forms in the lateral detection direction, where an equal and opposite change in rotation was observed with increasing L or D arabinose concentrations. The optical rotation was null in the exact backscattering direction, so this parameter is not sensitive to the presence nor to the isomeric form of the dissolved chiral species. This may be due to the retro-reflection of the beam along the same zig-zag path as the incident beam, inducing an equal and opposite counter-rotation and yielding a net measured rotation of ~0^o. Thus, although the polarization signal is present even in extremely scattering samples in this detection geometry, the measurable effect of chiral molecules may be weaker. That is, the presence of the chiral species is evident in both detection directions thru an increase in β, but the sense of the chiral asymmetry is not resolvable in retro-reflection (α~0 for both L and D isomers). Future work will investigate a possible compromise in polarization measurements slightly off the exact backscattering direction, where the polarization preservation will be less but the value of optical rotation may be non-zero.

Acknowledgements: This work was supported by funds from the Natural Sciences and Engineering Research Council (NSERC) of Canada. RDL and CW acknowledge the support of the Harold E. Johns Summer Studentship in Medical Physics at the Ontario Cancer Institute.

#696 - $15.00 US Received January 07, 2002; Revised February 21, 2002